Thematic set:
Messinian salinity crisis

PG
Petroleum Geoscience

Published Online First

doi:10.1144/petgeo2015-096

Seismic imaging of Late Miocene (Messinian) evaporites from Western Mediterranean back-arc basins

M. Dal Cin[1,2*], A. Del Ben[2], A. Mocnik[2], F. Accaino[1], R. Geletti[1], N. Wardell[1], F. Zgur[1] & A. Camerlenghi[1]

[1] OGS, National Institute of Oceanography and Experimental Geophysics, Trieste, Italy
[2] DMG, Department of Mathematics and Geosciences, University of Trieste, Trieste, Italy
* Correspondence: mdalcin@ogs.trieste.it

Abstract: An analysis of multichannel seismic reflection data was conducted focusing on the comparison between the Messinian Salinity Crisis (MSC) and Plio-Quaternary (PQ) evolution of the eastern Sardo-Provençal and northern Algero-Balearic basins and related margins in the West Mediterranean Sea. Both basins were completely opened during the MSC and their well-defined seismic stratigraphy is very similar in the deep parts. The primary difference between these two basins is due to their different pre-MSC extensional history, including the opening age and the stretching factors. These factors influenced the occurrence of post-MSC salt tectonics on these margins.

Received 22 December 2015; **revised** 19 July 2016; **accepted** 22 July 2016

The understanding of the Messinian Salinity Crisis (MSC) as a Mediterranean basin-wide event requires an improved knowledge of the stratigraphy in the deep basins and continental margins (e.g. Roveri *et al.* 2014). Due to the lack of lithological information from scientific and industrial wells, improvement of seismic imaging is currently the key element used to study the MSC stratigraphy in the deep basins, at least in academic seismic datasets (e.g. Lofi *et al.* 2011*a*).

In the Western Mediterranean, the geometry and distribution of the seismic markers of the MSC are not completely known due to uneven data distribution. In addition, seismic imaging is often hampered by deformation of the deep salt, high absorption and scattering of seismic energy by salt and other evaporitic formations, and high variability in seismic velocity across the salt sequence.

In this paper we focus on two recently acquired high resolution multi-channel seismic reflection datasets in the eastern Sardo-Provençal and northern Algero-Balearic basins (Figs 1 and 2). We have integrated the newer data with vintage seismic reflection profiles characterized by lower frequencies and higher penetration. Our aims are two-fold: (a) to test the possibility to improve the imaging of the sedimentary sequence and particularly of the seismic markers of the MSC affected by post-depositional deformation through accurate targeted seismic velocity analysis for pre-stack depth migration (PSDM); (b) to compare the structural and stratigraphic records of the two diachronous back-arc basins using the MSC sequence as a reference chronostratigraphic marker.

Geodynamic evolution and seismic stratigraphy

The Western Mediterranean region (Fig. 1) consists of several sedimentary basins evolved diachronously as back-arc response to the subduction of the Tethys Ocean lithosphere beneath the European plate to form the Apennines–Maghrebides Orogen during the Cenozoic (Cherchi & Montadert 1982; Gueguen *et al.* 1998; Carminati *et al.* 2012).

The first phase of the opening of the Western Mediterranean basins spans from the Early Oligocene (32 Ma, Carminati *et al.* 2012; 30 Ma, Cherchi & Montadert 1982; Rehault *et al.* 1984) to the Early Miocene (23 Ma, Cherchi & Montadert 1982; 21 Ma, Rehault *et al.* 1984; 22 Ma, Carminati *et al.* 2012), when continental back-arc rifting occurred with NE–SW strike in response to the northwestward subduction of the Tethys oceanic lithosphere below the European continental plate. This caused the clockwise rotation of the Balearic promontory and consequently the opening of the continental rift in the Valencia Trough.

In the Early Miocene (23 – 19 Ma, Cherchi & Montadert 1982; 22 – 15 Ma, Carminati *et al.* 2012; 21 – 18 Ma, Rehault *et al.* 1984; 21 – 16 Ma, Mauffret *et al.* 2004), the rifting progressively evolved eastwards to generate spreading of oceanic crust and led to the anticlockwise rotation of the Corso-Sardinian block that separated from the Balearic block through extensive right lateral motion along the North Balearic fracture zone (NBFZ). The formation of oceanic crust in the central Sardo-Provençal deep basin (Fig. 1) has been demonstrated through the identification of magnetic anomalies (Rehault *et al.* 1984), with magnetic and seismic reflection data (Fanucci & Morelli 2001) and with wide-angle and reflection seismic data (Afilhado *et al.* 2015; Moulin *et al.* 2015). The Sardo-Provençal basin is therefore considered a back-arc basin confined between the conjugated passive margins of the Corso-Sardinian micro-plate to the east and of the Gulf of Lions and Provence to the NW (Rehault *et al.* 1984; Fanucci & Morelli 2001; Finetti *et al.* 2005).

The Oligo-Miocene continental and open marine rift to drift deposits of the Sardo-Provençal basin were covered by the MSC evaporites and successively by the Plio-Quaternary (PQ) deep marine sediments. The present Sardo-Provençal abyssal plain is deepest (locally more than 2900 m) at the toe of the west Sardinian continental slope. This bathymetric trend is due to the large sedimentary influx from the Rhône and Ebro rivers, which feed large deep-sea fans prograding towards the east and SE. Due to the minor fluvial sedimentary supply, the deep-sea fans originated from the Corso-Sardinian continent are very small and steeper compared to the Rhône and Ebro fans.

The following rifting episode in the area was the opening of the Algero-Balearic basin (Fig. 1), separated from the Sardo-Provençal basin by the NW–SE-trending Hamilcar magnetic anomaly (HMA) (Mauffret *et al.* 2004; Driussi *et al.* 2015). In this case there are alternative geodynamic interpretations. According to some, rifting and seafloor spreading was triggered by the westward migration of the Gibraltar Arc from the Langhian (16 Ma) to the Tortonian

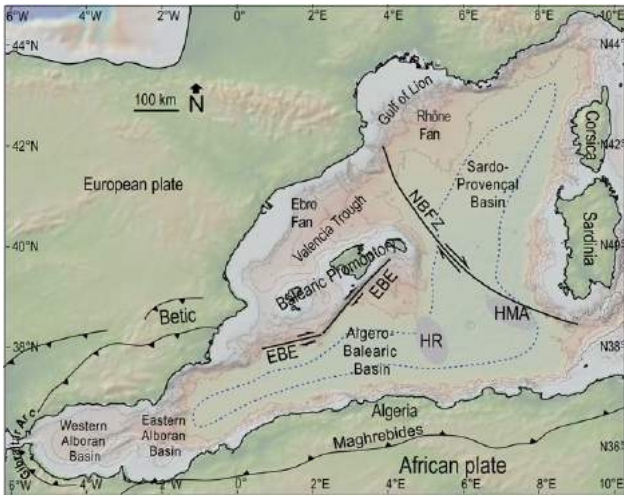

Fig. 1. Bathymetric map of the Western Mediterranean. The Sardo-Provençal basin is bound by the Corso-Sardinia (narrow shelf and steep slopes) and Gulf of Lion (wide shelf and gentle slope built by the Rhône deep-sea fan) conjugate continental margins (Rehault *et al.* 1984). The dextral strike-slip motion along the North Balearic Fracture Zone (NBFZ) allowed the Early Miocene anticlockwise rotation of the Corso-Sardinia block (Gueguen *et al.* 1998; Carminati *et al.* 2012). The northern margin of the Algero-Balearic basin (narrow shelf and steep slopes) is formed by a transform fault system (Emile Baudot Escarpment, EBE) (Acosta *et al.* 2001; Mauffret *et al.* 2004; Camerlenghi *et al.* 2009). Oceanic crust is present below the central parts of the deep basins (within the dashed line, according to Gueguen *et al.* 1998). The Hannibal ridge (HR) is considered the buried spreading centre of the oceanic Algero-Balearic basin (Mauffret *et al.* 2004). Black arrows indicate the direction of movement along the NBFZ and the EBE. The Hamilcar magnetic anomaly (HMA) (Mauffret *et al.* 2004) separates the Sardo-Provençal and the Algero-Balearic basins. Bathymetric contours are every 500 m.

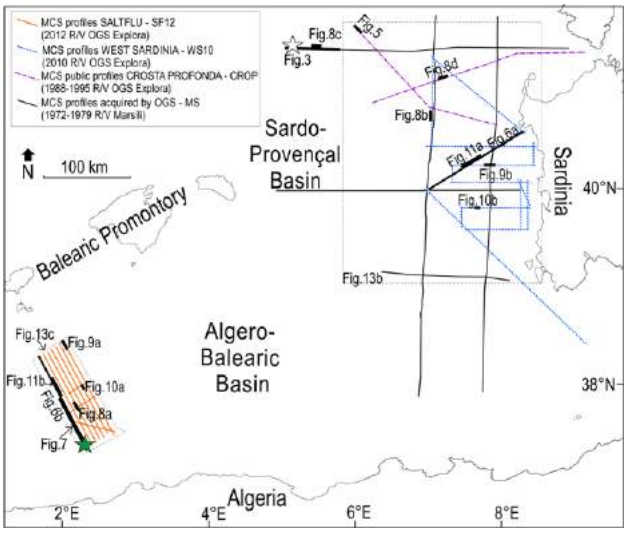

Fig. 2. Position map of the multichannel seismic reflection datasets used in this study. The recently acquired high resolution SF12 (solid grey (orange on pdf) lines) and WS10 (dotted (blue on pdf) lines) profiles were acquired specifically to address the MSC and later development of the Algero-Balearic and Sardo-Provençal basins and adjacent margins, respectively; the deep penetration of the older CROP (dot-dashed (violet on pdf) lines) and MS (solid black lines) were acquired to explore deep crustal structures at a regional scale. Bold black segments indicate position of the seismic profiles depicted in the figures of this paper. Rectangles with dot-dashed borders indicate the position of the isochron maps reported in Figure 13b and c. The dark (green) and white stars represent the position of the stratigraphic columns of Figure 12a and b, respectively. MCS, multichannel seismic.

(8 Ma) in an ENE–WSW direction (e.g. Driussi *et al.* 2015). Evidence for this is the identification of the north–south-trending Hannibal Ridge (HR), and associated magnetic anomalies, a relict and buried spreading centre with associated volcanic centres south of Menorca Island (Mauffret *et al.* 2004). Such direction of the Algero-Balearic basin opening is supported by the interpretation of the northern margin of the basin, marked by the Emile Baudot Escarpment (EBE), as a right-lateral strike-slip fault system generated in response to the westward migration of the Gibraltar Arc (Mauffret *et al.* 1992, 2004; Acosta *et al.* 2001; Camerlenghi *et al.* 2009; Driussi *et al.* 2015). Similarly the southern margin of the Algero-Balearic basin is defined by the North African continental margin, a rifted margin with dominance of left-lateral strike-slip deformation. This margin has been recently reactivated by active compressional deformation offshore Algeria (Déverchère *et al.* 2005; Domzig *et al.* 2006; Mauffret 2007). An alternative geodynamic model suggests that the accretion of the Middle Miocene oceanic crust occurred in a NW–SE direction as consequence of the eastward migration of the Apennines–Maghrebides arcs (Rehault *et al.* 1984; Gueguen *et al.* 1998; Carminati *et al.* 2012). According to Gallart *et al.* (1995) and Sàbat *et al.* (1995), the deep Algero-Balearic oceanic basement is covered by about 1800 m of Miocene sediments that include a deformed Messinian evaporitic sequence less than 1 km thick and a Plio-Quaternary sedimentary fill about 800 m thick.

There is general agreement that the Sardo-Provençal and the Algero-Balearic basins were both completely opened in the Tortonian (8 Ma) (Rehault *et al.* 1984; Gueguen *et al.* 1998; Mauffret *et al.* 2004; Carminati *et al.* 2012).

The MSC in the Mediterranean basin began shortly after, at 5.96 Ma (Krijgsman *et al.* 1999; CIESM 2008) and affected the whole Mediterranean region in the following 640 ka (Krijgsman *et al.* 1999; Roveri *et al.* 2014). This brief and dramatic event occurred in response to a tectonically driven reduced seawater exchange between Mediterranean and Atlantic waters (Clauzon *et al.* 1996; Krijgsman *et al.* 1999; CIESM 2008). Evaporites were deposited in the deeper basins, on the lower continental slopes and on several shallower marginal basins, whereas coeval erosion affected the intermediate and upper continental margins (Ryan *et al.* 1973; Butler *et al.* 1995; Clauzon *et al.* 1996; CIESM 2008; Roveri *et al.* 2014).

In the Western Mediterranean offshore, the seismic stratigraphic expression of the MSC is provided by a consistent succession of three seismo-stratigraphic units in the deep basins and lower slopes described for the first time in seismic profile MS-39 in the Sardo-Provençal basin (Finetti & Morelli 1973; Fig. 3). Seismic velocities obtained by Montadert *et al.* (1978) allowed the definition of three stratigraphic units (the 'Messinian Trilogy') that Rehault *et al.* (1984) subdivided into (from the bottom) the Lower Evaporites, Messinian Salt and Upper Evaporites. In this study we adopt the terminology proposed by Lofi *et al.* (2011*a*), who identified the Lower Unit (LU), Mobile Unit (MU) and Upper Unit (UU), respectively.

Additional Messinian surfaces are: the Bottom Surface/Bottom Erosion Surface (BS/BES) at the base of the MSC; the Intermediate Erosion Surface (IES) within the MSC; and the Top Surface/Top Erosion Surface (TS/TES) at the top of the MSC deposits.

On the upper continental slope, where the Messinian succession is generally absent, the Margin Erosion Surface (MES) is a prominent reflector corresponding to a hiatus in the entire MSC strata.

Locally, evaporite deposition occurred also on the upper continental slopes and shelves (Lofi *et al.* 2011*a*; Geletti *et al.* 2014), as well as in the present onshore regions (Cornée *et al.* 2008), probably during the first phase of the MSC (Butler *et al.* 1995;

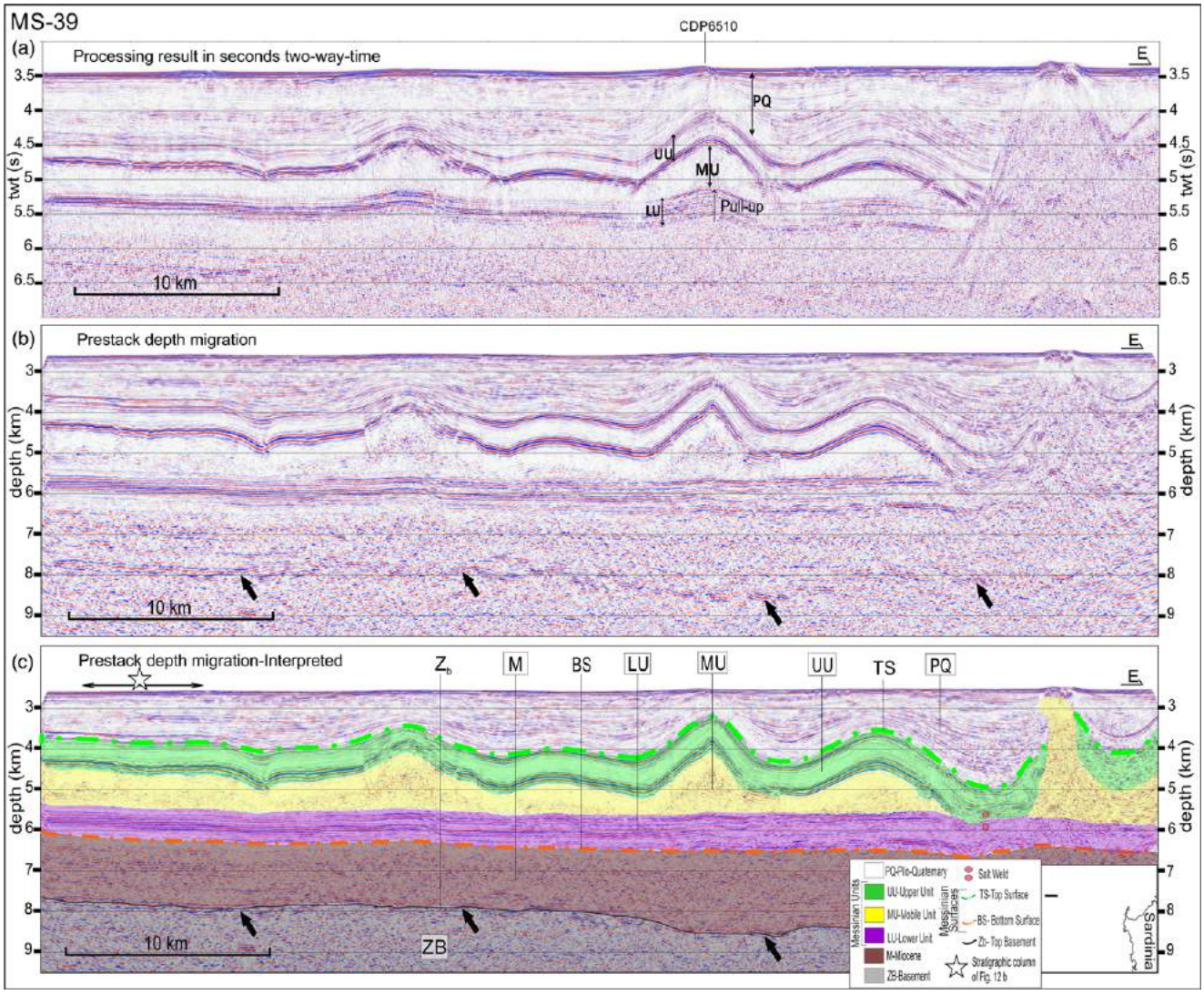

Fig. 3. Line MS-39 recorded by OGS (Finetti & Morelli 1973), in the Sardo-Provençal basin. The Messinian Trilogy (Rehault *et al.* 1984; Lofi *et al.* 2011*a*) is clearly imaged, from base to top: Lower Unit (LU), Mobile Unit (MU), Upper Unit (UU); along with non-erosive bottom and top surfaces (BS and TS, dot-dash lines, orange and green respectively in the pdf version). (**a**) Result of data processing in time domain: the pull-up event (dashed black arrow) of about 200 ms occurs beneath a MU dome and affects especially the LU. (**b**) Result of pre-stack depth migration (PSDM) showing flattened pull-up event. The velocity analysis shown in Figure 4 refers to CDP6510. (**c**) Interpretation of PDSM in (b): at around 8 km depth, the strong reflection (black arrows) has been interpreted as the top of the basaltic basement (Zb). Zb is overlain by the marine sediments (M) related to the drifting phase that led to the opening of the basin (Late Oligo–Early Miocene, Cherchi & Montadert 1982; Rehault *et al.* 1984; Mauffret *et al.* 2004; Carminati *et al.* 2012). Halokinesis of MU gives rise to domes that deform the overburden composed of UU and Plio-Quaternary units (PQ) and, locally, the seabed, indicating that the process is still active. The lower seismic facies of the PQ is characterized by well-layered and semi-transparent reflections of the Lower Pliocene (LP). PQ becomes progressively more reflective toward the top, where higher frequency reflections are ascribed to the Upper Pliocene–Quaternary (UPQ). Seismic images have the same horizontal scales; (b) and (c) are displayed with vertical exaggeration ×2.

Clauzon *et al.* 1996; Roveri *et al.* 2008). The seismic expression of these evaporites is defined as the Bedded Unit (BU), depicted by sub-parallel reflections and bounded by the TES and BES.

At the end of the MSC at 5.33 Ma, sea water refilled the Mediterranean basin and the Lower Pliocene (LP) pelagic sediments draped the margins extending to the entire Western Mediterranean basin (Ryan *et al.* 1973; Rehault *et al.* 1984) with a typical semi-transparent acoustic facies. The Upper Pliocene–Quaternary (UPQ) more reflective turbiditic layers correspond to coarse sediments deposited by European rivers (Rehault *et al.* 1984; Sage *et al.* 2005; Aslanian *et al.* 2012; Geletti *et al.* 2014).

Seismic datasets

The multichannel seismic reflection data used in this work were acquired in the framework of four research projects (Fig. 2): MS (Mediterranean Sea, Finetti & Morelli 1973), CROP (CROsta Profonda, Scrocca *et al.* 2003; Finetti 2005), WS10 (West Sardinia, Geletti *et al.* 2014) and SF12 (Eurofleets project Salt deformation and sub-salt Fluid circulation – SALTFLU). The MS and CROP regional projects covered extensive areas of the Mediterranean, while WS10 and SF12 were targeted to specific regions. The WS10 dataset consists of 15 multichannel seismic profiles in the eastern sector of the Sardo-Provençal basin and adjacent passive margin, the SF12 dataset consists of 10 multichannel seismic profiles in the northern sector of the Algero-Balearic basin and adjacent passive margin. Location and seismic acquisition parameters of each survey are reported in Figure 2 and in Table 1, respectively. During the WS10 and SF12 projects, sub-bottom profiles and multibeam bathymetry were also acquired.

The WS10 and SF12 profiles were acquired with the specific aim of investigating the Messinian and post-Messinian sedimentary

Table 1. *Acquisition parameters of the available datasets in the Western Mediterranean Sea*

Project name	WS10 OGS lines	CROP Public lines	SF12 OGS lines	MS OGS lines
Line name	WS10–01 to WS10–15	CM1, CM2A	SF12–03 to SF12–12	MS39, MS40, MS43, MS44, MS95
Vessel	*OGS Explora*	*OGS Explora*	*OGS Explora*	*Marsili*
Recording date	2010	1988, 1991	2012	from 1972 to 1979
Recorder	Sercel Seal	Sercel SN 358 DMX	Sercel	T.I. DFS/10.000
Sample rate (ms)	1	4	2	4
Field filters	Low 3 Hz, high 500 Hz	Low 8 Hz, high 77 Hz	Out–out	Low 10 Hz, high 72 Hz
Max coverage	30	30, 45	60	12, 24
Energy source	GI-gun Sercel	Air guns	GI-gun Sercel	Flexotir
Dominant (Hz) source frequency	150	60	200	100
Source array	1 × 2 guns = 710 cubic inch	4 × 8 guns = 5000 cubic inch	2 × 4 gunsx210 = 1680 cubic inch	3 guns, microcharges of 50 g, Geodin - B
Depth of source (m)	4	6	3	14
Streamer (m)	1500	3000, 4500	3000	2400
Number of traces	120	120, 180	240	24
Group interval (m)	12.5	25	12.5	100
Shot interval (m)	25	50	25	100, 50
Depth of streamer (m)	5	12	4	10
Near offset (m)	25	170, 150	25	320

sequences. With this aim the acquisition parameters were chosen with a good compromise to obtain satisfactory resolution and sufficient penetration. The MS and CROP data were acquired with the purpose of investigating the deep crustal structure; thus they allowed us to define the basement and, locally, the lower crust and the Moho.

We calculated the theoretical vertical resolution for each dataset according to the λ/4 (where λ is the seismic wavelength) Rayleigh criterion (Kallweit & Wood 1982) and considering the maximum source frequency listed in Table 1 and an average seismic velocity of 2000 m s^{-1} for shallow, post-MSC sediments. SF12 and WS10 datasets are characterized by a vertical resolution of 2.5 m

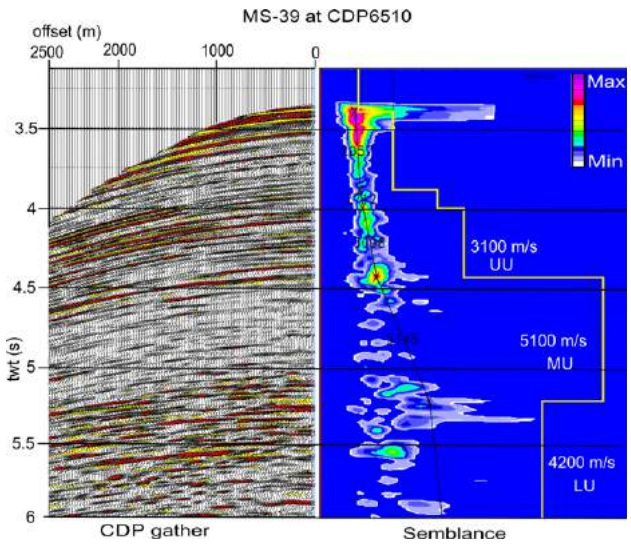

Fig. 4. Velocity spectrum analysed on Semblance panel from Common Mid Point Gather (CMP, time domain) of profile MS-39 (CDP 6510, location in Fig. 3a). Interval velocity of Upper Unit (UU), Mobile Unit (MU) and Lower Unit are, respectively, about 3100 m s^{-1}, 5100 m $s^{-1}$and 4200 m s^{-1}. The interval velocity of 5100 m s^{-1} for MU is higher with respect to the mean value of about 4500 m s^{-1} provided by Montadert *et al.* (1978) on the same line. PSDM with MU interval velocity of 5100 m s^{-1} yields a complete flattening of the base of salt, compensating for the velocity pull-up effect of the section processed in time domain (see Fig. 3).

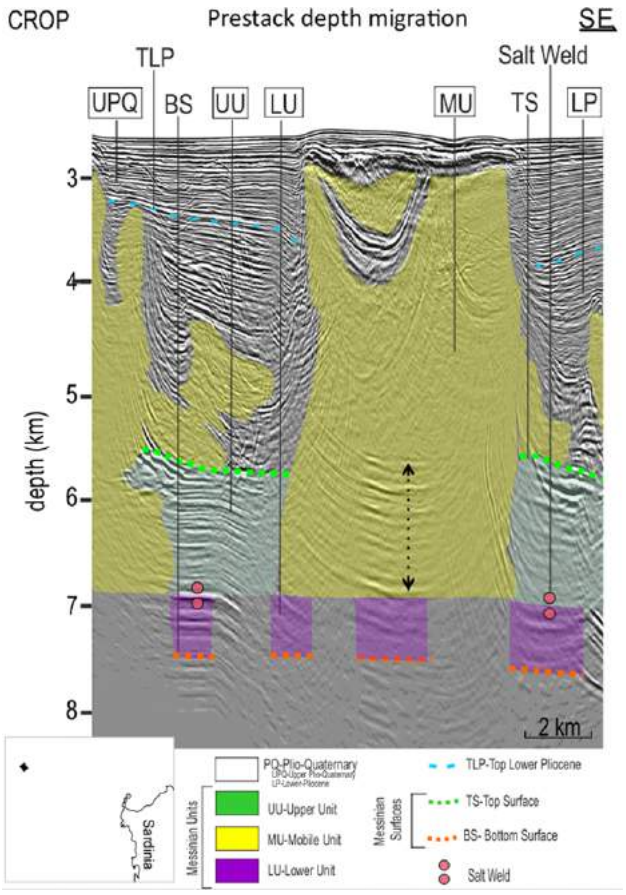

Fig. 5. Pre-stack depth migration of part of the profile CROP in the NW Sardo-Provençal basin, showing the typical seismic facies of the Messinian Trilogy. The diapir, which is almost 4000 m high, intrudes almost entirely the Plio-Quaternary (PQ) sequence, inducing deformation of the seabed. The lateral flow of the salt feeding the big diapir has formed salt welds (solid circles). The PQ sequence overlaying the top of the diapir is about 500 m, while around it the PQ is almost 3000 m. The bottom (BS) of the Lower Unit (LU) reaches 7.4 km of depth. The dashed arrow indicates a package of reflections that we ascribe to stratified Upper Unit (UU) incorporated during halokinesis or to lateral seismic events.

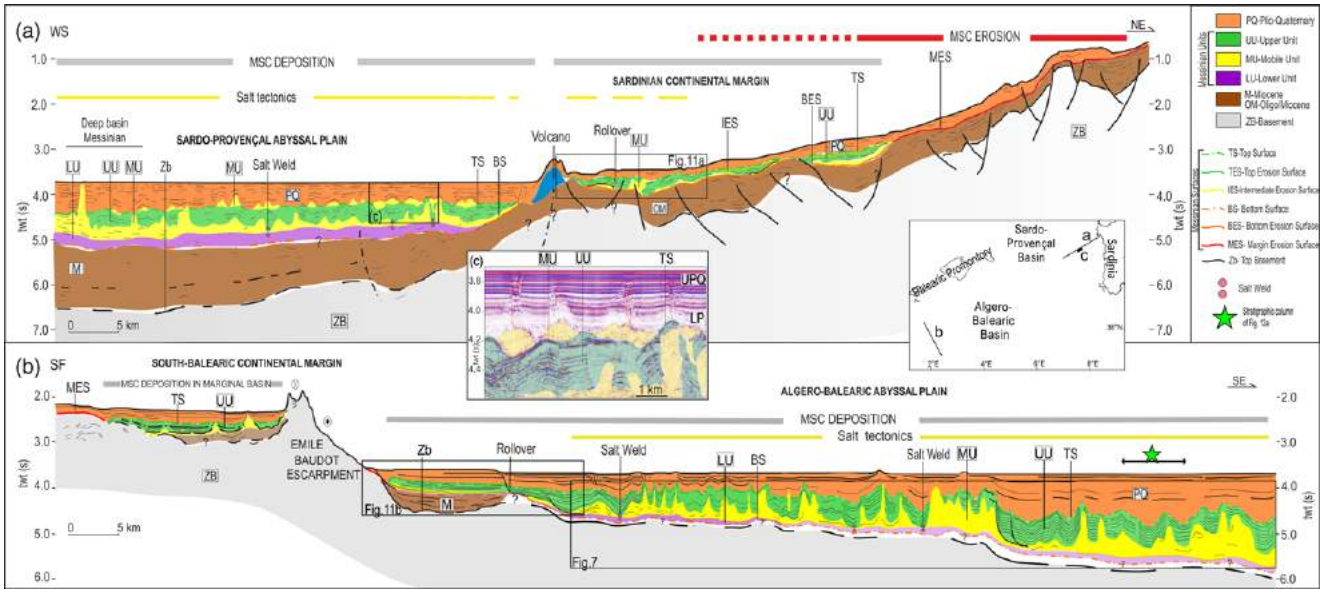

Fig. 6. Comparison between two representative profiles across the two investigated margins. (**a**) WS10 data of the west Sardinian margin and adjacent eastern Sardo-Provençal abyssal plain. (**b**) SF12 data of the south Balearic margin and adjacent northern Algero-Balearic abyssal plain. Despite the diachronous origins, both the basins were completely open at the onset of the MSC: their Messinian to Quaternary evolution is thus comparable, as suggested by similar thicknesses of the MSC and PQ units. The Messinian Trilogy is present in both the deep basins and generally thins toward the continental margins with onlapping terminations. Salt deforms and intrudes the overlying UU and Plio-Quaternary (PQ) sequences. Growth strata in the UU indicate that halokinesis locally began during deposition of UU in both the basins. In the Sardo-Provençal basin (a) halokinesis commonly creates allochthonous bodies of MU at the lithological discontinuity between UU and LP (see inset (**c**)). Salt rollover structures are common on the lower slope of the Sardinia margin. Thin UU and MU, often bordered by the erosional surfaces BES and TES, gradually disappear on the upper slope and they laterally converge to the MES. The structure of the Algero-Balearic continental margin is characterized by a steep fault scarp that separates a marginal slope basin from the deep basin. Deep MSC units onlap at the foot of the fault scarp (see also Fig. 11) with quite rare rollover structures; (a) and (b) are displayed with the same vertical and horizontal scales.

and 3 – 4 m, respectively. MS and CROP datasets provide a vertical resolution of 6 – 7 m and 8 m, respectively.

The available multichannel seismic data were processed using Echos and Geodepth software from Paradigm Geophysical. The applied processing sequence can be summarized as follows: trace editing, spherical divergence correction and absorption compensation, predictive deconvolution, normal move-out correction (NMO) with stacking velocities (obtained after iterative analysis and interpretation of Common Offset Sections), stretch muting, stacking, time variant filtering and post-stack time migration. PSDM on selected parts of MS and of CROP (processed by Dal Cin 2014) provided information on interval velocities of MSC units through velocity spectra analysis (on Common Depth Point, CDP, Gathers and Semblance panels).

Results

Deep basins

In the oceanic domain of the Sardo-Provençal basin the deep penetration of MS and CROP profiles allows imaging of the entire stratigraphy, particularly in areas with weak halokinesis (Fig. 3). Application of PSDM on selected segments of data allowed us to obtain reliable interval velocities within MSC and PQ units (Fig. 4). The interval velocity of 5100 m s^{-1} for MU may appear relatively high with respect to the mean value of about 4500 m s^{-1} provided by most Messinian studies from both the West and East Mediterranean (e.g. Montadert *et al.* 1978; Lofi *et al.* 2011*a*, *b*). The interval velocities of the Levant Basin MU are even lower (Costa *et al.* 2004; Reiche *et al.* 2014; Feng & Reshef 2016), as the salt is intercalated with clays (Feng & Reshef 2016). Studies based on laboratory experiments (Jones & Davison 2014) report pure halite seismic velocities of 4500 m s^{-1}, gypsum and anhydrite velocities of 5700 m s^{-1} and 6500 m s^{-1}, respectively. On the other hand, potassium and magnesium salts, often associated with halite, have lower velocity than halite. An erroneous picking of the lower and upper MU boundaries that includes reflectors from the gypsum composing LU and UU can be excluded. In the absence of lithological information for the deep basin Messinian evaporites in the Western Mediterranean, we infer that a certain amount of high velocity gypsum or anhydrite is present within the main halite body in this area. This mineral composition of salt layers is present in various evaporite-bearing basins, revealing velocities values higher than 4500 m s^{-1} (Jones & Davison 2014). Moreover, Decima & Wezel (1971) and Roveri *et al.* (2008, 2014) report the presence of gypsum within the salt unit in the Messinian deep marginal basin in Sicily, that is considered the best onshore analogue of the unsampled Messinian Trilogy in the deep Western Mediterranean basins. We propose that PSDM with MU interval velocity of 5100 m s^{-1} yields a complete flattening of the base of salt (Fig. 3b,c), compensating for the velocity pull-up effect of the section processed in time domain (Fig. 3a). In the Sardo-Provençal deep oceanic basin, the top of basaltic basement (Zb) is recognized at a depth of *c.* 8 km below the sea surface (*c.* 5.1 km below the seafloor) and is overlain by a pre-MSC sequence about 1.7 km thick characterized by poor lateral continuity of reflectors and, in general, reflector strength increasing with depth. The oceanic basement shows moderate relief not exceeding 500 m in the section imaged in Figure 3b and c.

The oceanic basement is not imaged in the data from the Algero-Balearic basin, as penetration of acoustic energy is highly hampered by intense halokinesis.

The three MSC seismostratigraphic units are clearly imaged in the Sardo-Provençal basin (Fig. 3).

LU, MU and UU lay conformably above the pre-MSC sequence. LU, highly reflective, displays an increasing thickness

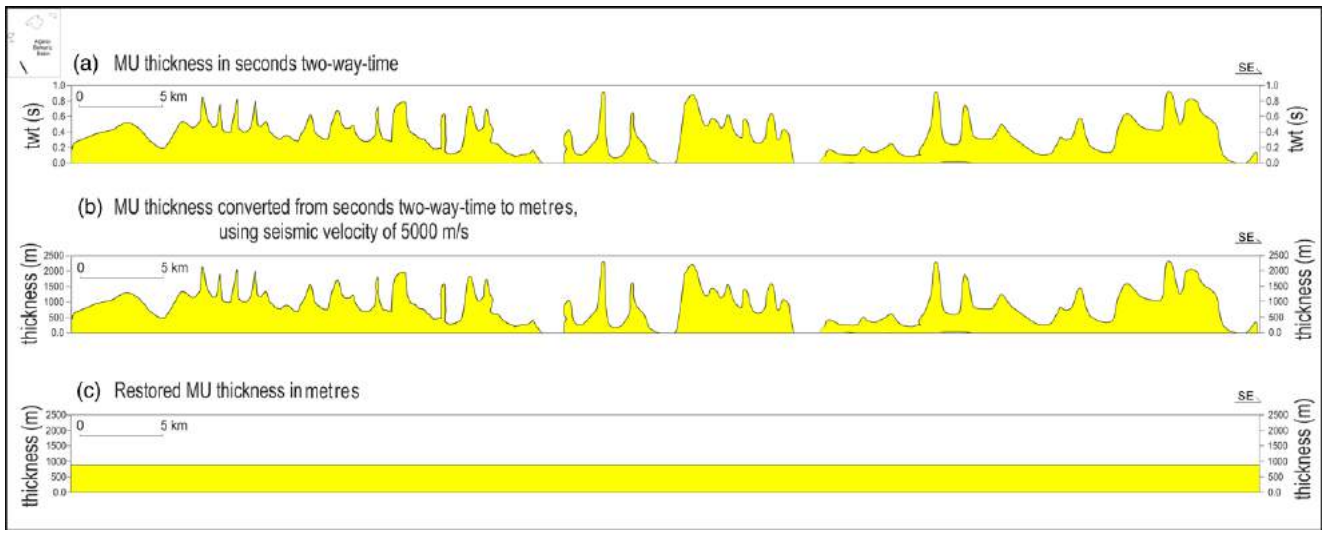

Fig. 7. Qualitative evaluation of the original MU thickness from line SF12 in the Algero-Balearic basin (Fig. 6). (**a**) Thickness in twt (s) of the deformed MU corresponding to that within the black rectangle in Fig. 6); (**b**) converted thickness of deformed MU section (a) into depth by using mean interval velocity of 5000 m s^{-1}. (**c**) Restored MU, along the same length as (a) and (b), resulting in an average thickness of *c.* 900 m. (a–c) have the same horizontal scale; (b and c) have the same vertical scale. Using a mean interval velocity of 4200 m s^{-1} for MU (calculated by Costa *et al*. 2004; Reiche *et al*. 2014; Feng & Reshef 2016 for the Eastern Mediterranean MU) or of 4500 m s^{-1} (calculated by Montadert *et al.* 1978 for the Western Mediterranean deep basin MU) the thickness of restored MU would be about 700 m and 800 m, respectively.

from 700 m to about 1 km from west to east, produced by westward reflector divergence. MU is reflectorless with a thickness of about 1 km where undeformed. UU is about 800 m thick and displays high reflectivity except in its upper and lower boundaries. The base of LU occurs at a depth of 3.4 km below seafloor in the undeformed sequence (Fig. 3b and c), possibly deeper if correctly interpreted between salt structures (Fig. 5). Like the oceanic basement, LU is also not recognizable in the dataset from the Algero-Balearic basin other than in a very tentative way due to diffuse halokinesis.

MU often shows chaotic reflections that we ascribe to incorporation of portions of layered sequences during halokinesis or to lateral seismic events (Fig. 5). The thickness is highly variable, with a decreasing thickness trend approaching the Sardinian margin from the west (Fig. 6a). The nature of the eastward-thinning salt is unclear due to the lack of internal reflectors. Salt is expected to thin

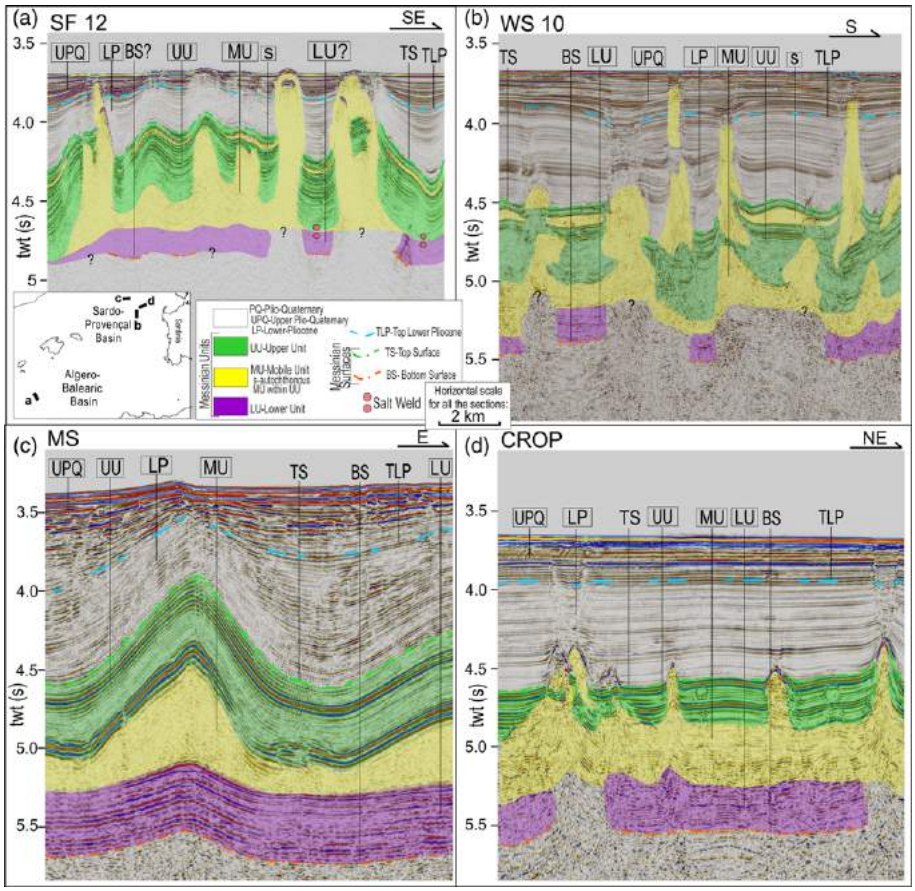

Fig. 8. Typical deep basin salt structures imaged with different vertical resolution by the four seismic datasets analysed in this study. Seismic images refer to (**a**) the north Algero-Balearic and (**b–d**) the Sardo-Provençal basins. The high resolution of both the SF12 (a) and WS10 (b) datasets allows a clear identification of Plio-Quaternary (PQ) and MSC reflectors. Note the thin transparent autochthonous salt layer 's' identified within the Upper Unit (UU). (a and b) show UU composed of an upper alternation of 9–10 high/low amplitude events and a lower low amplitude package. Deep penetration MS (c) (modified, Finetti & Morelli 1973) and CROP (d) data give images of LU base and deeper reflections. In both basins MU generates diapirs piercing the UU and the PQ. PQ is composed of a low amplitude Lower Pliocene (LP) layer overlain by a high amplitude Upper Plio-Quaternary (UPQ) package. In (a and c) note the onlap and pinch-out terminations inner and above the top of the LP (TLP), suggesting that halokinesis was often active during the entire Pliocene. The process is still active as testified by seabed deformation induced by the largest diapirs. Seismic images have the same vertical and horizontal scales.

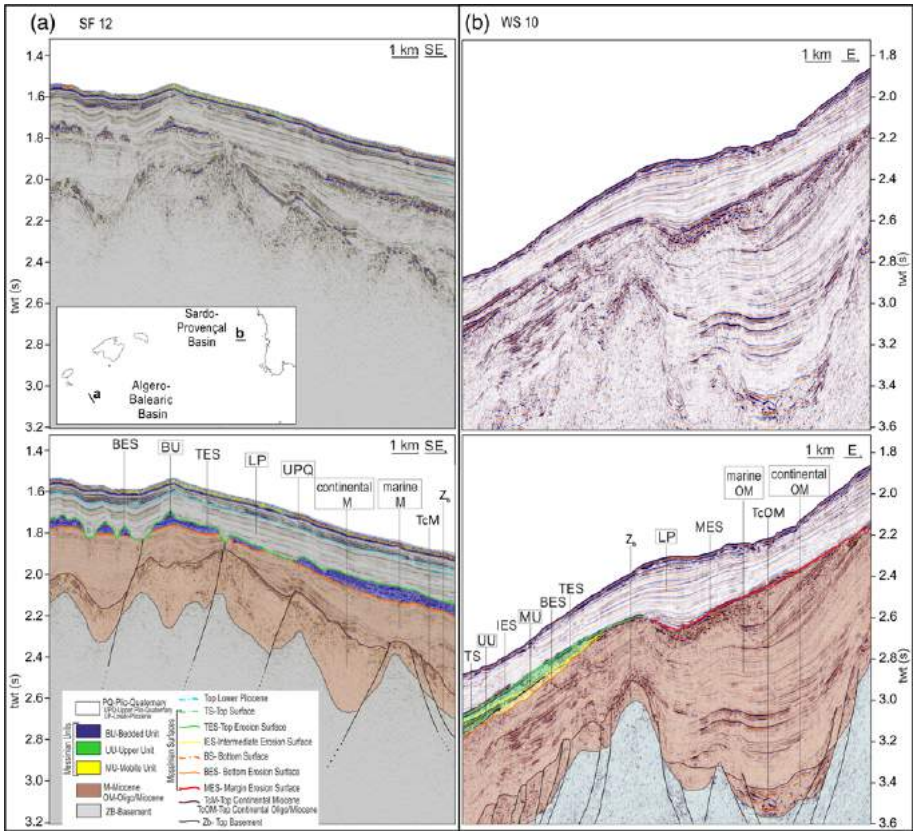

Fig. 9. Comparison between (**a**) the south Balearic and (**b**) western Sardinian continental margins (modified from Mocnik *et al.* 2014). The basement is cut by faults produced by the Oligo-Miocene rifting phases. Horst and graben are filled by continental syn-rift (cOM, cM) deposits with high amplitude seismic response and chaotic internal configuration. Post-rift marine (mOM, mM) deposits are characterized by subparallel continuous and low amplitude seismic packages. (a) In the south Balearic margin the top of the mM is erosive and is overlain by high amplitude packages that we ascribe to the Messinian Bedded Units (BU) (Lofi *et al.* 2011*a*). BU is bounded by erosional surfaces at its bottom (BES) and top (TES). The Plio-Quaternary (PQ) sequence directly overlies the TES. (b) In the west Sardinian margin the thin MU and UU are present on the lower slope. Their lower boundary BES represents the erosional truncation of the mM unit. The upper boundary of the UU is the TES and an erosion surface IES is also present within it. In the upper slope the Messinian units converge in the margin erosion surface MES. The MES truncates the post-rift units and is covered by the LP semi-transparent unit. Also the current seafloor is affected by erosion that origins irregular morphology. Seismic images (a) and (b) have the same vertical and horizontal scales.

towards the edge of the evaporitic basin due to lateral onlap. Salt redistribution towards the basin centre may have equally contributed to such thinning.

Interestingly, part of the salt has risen diapirically through the UU and has spread laterally at the base of the Plio-Quaternary sequence forming smaller-scale salt structures (Fig. 6a and c). Because such structures have induced folding in the Plio-Quaternary strata, we infer that salt intruded along the discontinuity between UU and the overlying Lower Pliocene sediments favoured by the changing mechanical properties between indurated gypsum and overlying soft deep-sea clay-rich muds.

In the Algero-Balearic deep basin MU is imaged in a variety of structures and its base can be traced with discontinuity (Fig. 6b). Starting from the deep basin salt distribution interpreted on the seismic profile of Figure 6b, we have converted MU traced in two-way travel times to depth using a mean interval velocity of 5100 ms^{-1}, and

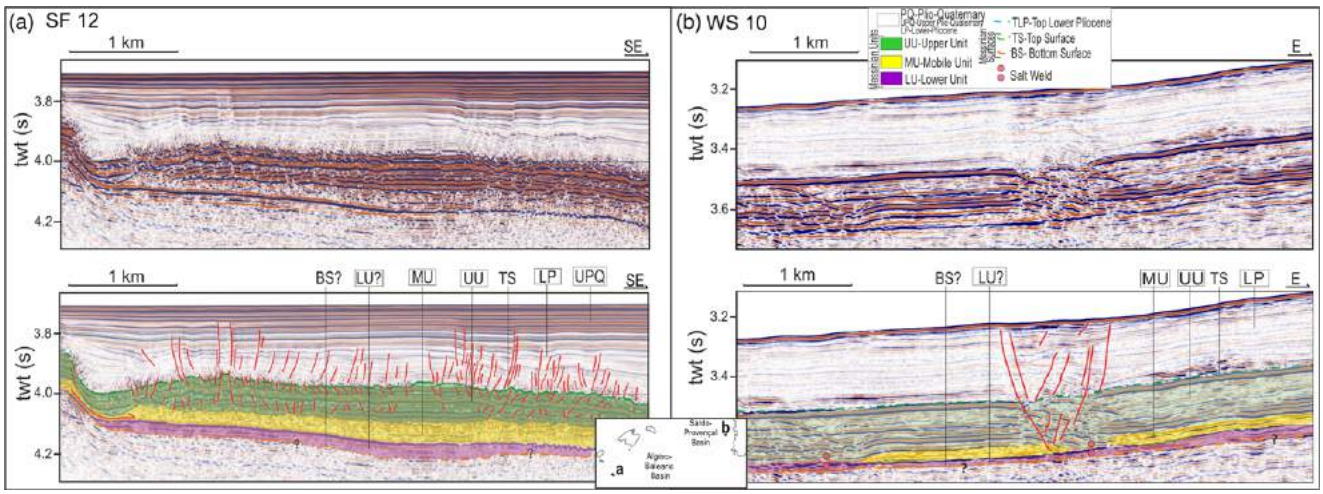

Fig. 10. Comparison between MSC deposits in (**a**) the Algero-Balearic basin (modified from Wardell *et al.* 2014) and (**b**) the Sardo-Provençal lower slope. Analogies can be recognized in terms of thicknesses and seismic characters of the Messinian Trilogy, which shows its typical seismic facies: the UU (about 150 ms twt thick) package of high/low amplitude alternation, the thin, semi-transparent MU and the thin, highly reflective LU. Seismic images have the same vertical and horizontal scales. The fault pattern affecting UU, especially on the Balearic margin, has been interpreted as volumetric change induced by gypsum to anhydrite transformation and dewatering that propagates into the overlaying Plio-Quaternary muds.

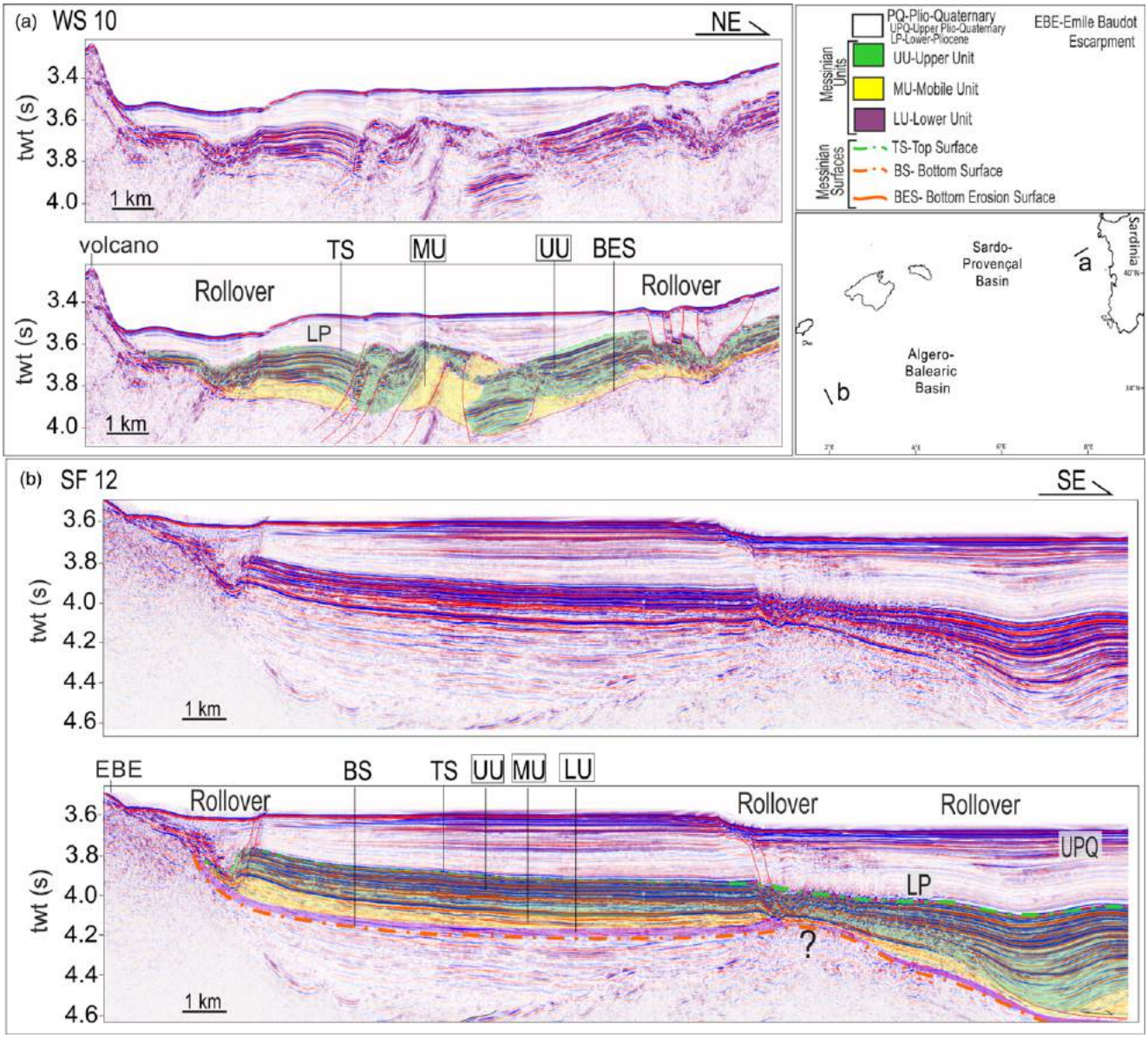

Fig. 11. Salt rollover structures on the lower slopes of the Sardinia and Balearic slopes. (**a**) Profile WS 10 from the Sardinian margin. The lateral continuity of MU from the deep basin to the continental slope has promoted the salt detachment and generation of pervasive rollover structures also in marginal slope basins. (**b**) Profile SF 12 from the Balearic margin. Rollover structures are rarely observed. In this case they form at the transition between the lowermost slope basin and the deep basin, where thin salt has detached towards the deep basin. Further up-slope the MSC units onlap against the EBE fault escarpment, on the left. Both profiles are displayed with the same horizontal and vertical scale. See text for discussion.

finally we have averaged the salt thickness to obtain a uniform layer resulting *c.* 900 m thick (Fig. 7). This procedure suffers from approximations induced by uncertain picking of the base of UU and lateral salt flowage affecting its thickness in the analysed cross-section. The resulting restored thickness of the halite layer is, however, strikingly similar and comparable to the 1 km thickness one observed in the undeformed Sardo-Provençal deep basin (Fig. 3).

In both basins salt structures generally induce folding and often pierce through the overlying gypsum and marls (UU) and the Lower Pliocene deep-sea muds (LP). Less frequently they cause intense deformation in the UPQ units and breach through the sea bottom (Figs 3, 5, 6 and 8). The lateral spread of salt at the base of the Plio-Quaternary sequence observed in the Sardo-Provençal basin is not observed in the Algero-Balearic basin.

Similarly to the Sardo-Provençal basin, incipient halokinesis had already locally begun during the deposition of UU in the Algero-Balearic basin (e.g. Fig. 6). Salt deformation proceeded more intensely during the Early Pliocene, as suggested by frequent onlap or pinch-out terminations of high amplitude above the Lower Pliocene semi-transparent reflectors (Fig. 8a–c). A progressive attenuation of salt deformation occurred in the Upper Pliocene–Quaternary (UPQ unit). However, some morphological features on the seafloor of both the basins testify that locally the process is still active (Figs 3, 5 and 8a). UU, where undeformed, attains a rather uniform thickness of about 800 m in both the basins, while it displays highly variable thickness as a consequence of syn-sedimentary halokinesis. A semi-transparent layer within the upper part of UU has been highlighted in the Sardo-Provençal basin (Fig. 8b), which has been labelled ‘s’ according to Geletti *et al.* (2014). Internal configuration and geometry of the ‘s’ layer suggest it is composed of salt. It rarely exceeds the thickness of 15–20 ms twt (about 50 m, using a seismic velocity of 5100 ms^{-1}). The same layer is also found in the Algero Balearic basin (Fig. 8a), but thinner and without the marked doming structure found in the Sardo-Provençal basin. Due to insufficient vertical resolution the ‘s’ layer is not observed in CROP and MS profiles (Fig. 8c and d).

Above the Messinian sequence the Lower Pliocene (LP) is marked by a low reflectivity unit commonly referred to muds deposited after the re-establishment of open marine conditions at the base of the Pliocene (Hsü *et al.* 1973; Rehault *et al.* 1984; Lofi *et al.* 2005; CIESM 2008). LP is overlain by a package of higher intensity reflectors related to turbiditic bodies which deposited during the UPQ. Normal faults can be generally identified above the salt diapirs (Fig. 8). The thickness of the Plio-Quaternary sediments appears to be an important factor in generating the salt structures. In both basins the largest diapiric structures are present in the areas of the Plio-Quaternary depocentres (Figs 5 and 6). In the Sardo-Provençal basin this is in the NW of the basin, while in the Algero-Balearic basin it is in the southern part (see isochron maps of Fig. 13b and c).

Lower slopes

LU, MU and UU are found on both the south Balearic and western Sardinian lower slopes, where they thin and eventually disappear (Figs 6, 9–11). In many places the current termination does not represent the original depositional termination, as salt detachment and flow toward the basin have displaced the termination basinward (Fig. 6). Rollover structures (Figs 6 and 11) are particularly evident on the conjugate margins of the Sardo-Provençal basin (e.g. Sage *et al.* 2005; Lofi *et al.* 2011*a*; Geletti *et al.* 2014) as a response to a progressively increasing slope angle of a subsiding continental margin loaded by terrigenous sedimentary input. Salt flow toward the basin is less represented in the data of the northern margin of the Algero-Balearic basin, with rare and weaker rollover structures. The right-lateral tectonic imprint on the basin margin defined by the steep Emile Baudot Escarpment emplaced before the MSC, combined with the very limited fluvial contribution to the sedimentary budget from the Balearic promontory, have not created the geological conditions favourable for the large-scale development of salt rollover structures.

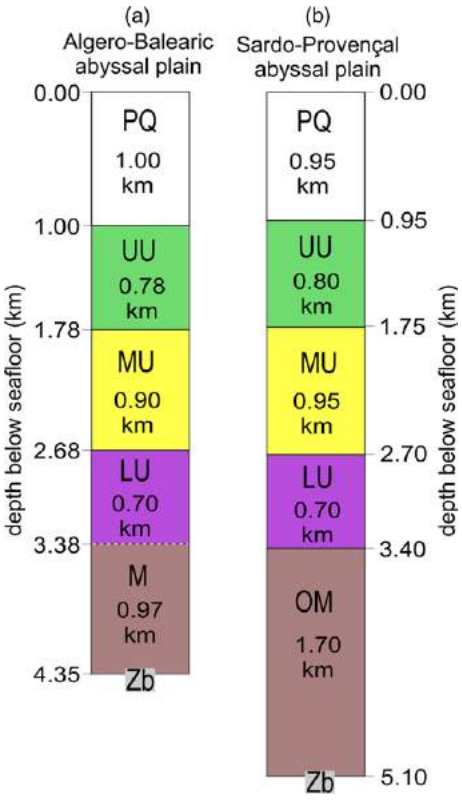

Fig. 12. Representative stratigraphic columns of the deep (**a**) Algero-Balearic and (**b**) Sardo-Provençal basins. The two columns have been deduced by (**b**) the PSDM MS-39 profile in Figure 3 and by (**a**) depth conversion of part of the profile in Figure 6 using the velocity analysis performed through PSDM (Fig. 4). In the Algero-Balearic basin, where the deep basin sequence is always intensely deformed, the original thickness of the MU has been restored (Fig. 7). Both basins are today at a similar water depth and have remarkably similar MSC and Plio-Quaternary sequences. The striking difference is the thickness of the pre-MSC sequence and, therefore, the depth of the oceanic basement. This difference is likely due to the different age of oceanic spreading in the two basins.

LU can be traced upslope in both deep basins and margins as a thin (some tens of milliseconds twt), highly reflective, layer (Figs 6 and 10). The overlaying MU is often deformed, particularly in the Sardinian slope, with salt flow creating salt weld surfaces, block faulting, rollover and sliding of the UU that seems partially still active (Fig. 6, 11a). UU has the typical seismic character represented by an alternation of 9–10 closely spaced high amplitude reflectors (Figs 10 and 11). This yields a thinner UU sequence overlying a thinner MU compared to the deep basins. In the time domain the thicknesses of UU range between 0 and 250 ms (0 – 390 m from PSDM), and the UU top is generally deeper in the Balearic margin (about 3.9 s twt) than in the Sardinian margin (3.45 s twt). The lateral continuity between LU, MU and UU suggests that during the MSC there was a clear connection between the deep basins and the lower slope basins, where very similar evaporitic sequences in the seismic record were deposited in very different water depths (Fig. 6).

On both continental margins, the Plio-Quaternary is represented mainly by the LP sequence, while only a thin high amplitude reflector package, when present, can be ascribed to the UPQ (Figs 9, 10a and 11b). The total thickness ranges between zero and *c.* 300 ms twt. The lower boundary of PQ is represented by the TS conformity that locally becomes erosional (TES). On the middle/upper slope the entire MSC is represented by an erosional hiatus (MES) (Figs 6 and 9). The seafloor of the southern Balearic margin is affected by erosion by down-slope sediment transport along the steep EBE (Fig. 6b). The seafloor of the Sardinian margin shows erosional effects by bottom currents and turbidity currents (Geletti *et al.* 2014; Fig. 9b).

Discussion

In Figure 12 we present a one-dimensional synthesis of the seismically-derived stratigraphy of the Sardo-Provençal and Algero-Balearic basins. They have been obtained from prestack depth migration and conversion to depth, respectively.

The abyssal plains of the Sardo-Provençal and Algero-Balearic basins lay at a comparable water depth as they belong to the same Quaternary deep-water turbidite sedimentary system. The main depocentre in this sedimentary system is the Rhone deep-sea fan, outside the area covered by the datasets analysed in this work. The oceanic basement is clearly identified at *c.* 6.5 s twt in the Sardo-Provençal basin (5.1 km after PSDM; Fig. 3), deeper than the weakly, though consistently identified oceanic basement top at about 5.8 s twt in the Algero-Balearic basin (Fig. 6b and ESCI Profile across the Valencia Trough, Sàbat *et al.* 1995). Using a similar seismic velocity structure as in the Sardo-Provençal basin (Fig. 4), the depth of the basement in the Algero-Balearic basin is about 4.35 km below the seafloor.

The MSC seismo-stratigraphic units appear very similar in both deep basins. The thickness of MU (measured where undeformed, or restored) is consistent between 0.9 and 0.95 km. UU, where undeformed, is about 800 m thick in both basins. Uncertainty is only about the thickness of LU. In the Algero-Balearic basin there is a marked increase in LU thickness towards the margin, due to reflector divergence probably produced by terrigenous input from

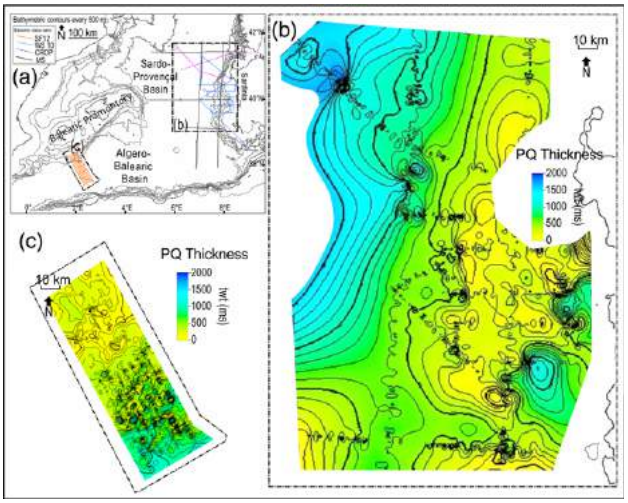

Fig. 13. Isochron maps performed from the interpreted Plio-Quaternary (PQ) sequence on the available seismic datasets: (**a**) bathymetric map and position of the available seismic profiles in the Western Mediterranean. (**b**) Thickness map (twt) of the PQ in the Sardo-Provençal basin (with values that regionally increase toward the NW. (**c**) Thickness map (twt) of the PQ in the Algero-Balearic basin with values that increase southeastward. Local trends, in both the maps, are related to the presence of salt diapirs. Maps in (b and c) have equivalent scales that are proportionally enlarged with respect to the scale of the map in (a) and equal contour intervals of 200 ms twt.

the Sardinian margin during deposition of the lower evaporites. However, because LU shows remarkable similarity between lower slope basins in the two margins, we can assume that the same similarity applies to LU in the deep basins.

The thickness of the PQ is 0.95 – 1 km in the deepest part of both basins.

The different depth of the oceanic basement depends on the different thickness of the pre-MSC formations resulting from the different opening ages of the two basins. The time elapsed between the end of the rifting phase and the end of the MSC is 17 Ma for the Sardo-Provençal margin and 10 Ma for the Algero-Balearic margin, resulting in a pre-MSC sequence thickness of 1.7 and 0.97 km, respectively. At the onset of the MSC the basin floors were already filled with a uniform sedimentary layer. Evaporitic deposition during the MSC was even across the two basins, with minor lateral changes in LU in response to local terrigenous sediment input from the Sardinian margin. According to the post-rift thermal subsidence curve (McKenzie 1978), the younger Algero-Balearic basin should have subsided more rapidly than the Sardo-Provençal basin provided the stretching factor ß was the same. The fact that the MSC and later evolution of the sedimentary fill is absolutely comparable in the two basins can be explained with a stretching factor in the Algero-Balearic basin lower (therefore with a lower subsidence rate) than the high values of 10 and 3 – 7 proposed for the Sardo-Provençal basin by Steckler & Watts (1980) and Rehault *et al.* (1984), respectively.

Among the three MSC seismic units, UU is the one that is better imaged in the analysed data and provides two distinctive characters for the two basins. The intra-UU salt layer 's' is present in the deepest part of both basins, with a greater thickness in the Sardo-Provençal basin. The event that caused salt deposition towards the end of the MSC, while the upper evaporite gypsum and clastics were deposited in the deep basins, can be considered a regional event in the Western Mediterranean. The reason for the 's' layer not being identified in other parts of the Western Mediterranean is probably two-fold: (1) the relatively high resolution of the deep-water seismic survey of the datasets analysed in this study; and (2) the possible dilution of gypsum and salt by clastics in the peripheral areas of the Western Mediterranean, with particular reference to the Gulf of Lion depocentre where most of the available information comes from. Following the MSC evolutionary model of Rouchy & Caruso (2006), Ryan (2008) and Lofi *et al.* (2011*b*), we infer that the deposition of the 's' layer followed a second, short decrease in the base level. This secondary base level drop is correlatable to the intra-UU erosion (IES), which is well defined on the Sardinian continental slope (see also Geletti *et al.* 2014). Such unconformity is not present on the South Balearic margin, because the margin is produced by a large tectonic structure pre-dating the MSC that has segmented the margin in isolated marginal slope basins separated by steep fault-scarps where no MSC evaporites could accumulate. The lateral continuity of the MSC units from deep basin to slope is missing, and the IES is not preserved in the sedimentary record.

The main salt body MU of the MSC is imaged undeformed only in the distal part of the Sardo-Provençal basin. Elsewhere in the deep basins it is deformed by various diapiric structures in the deep basins and rollover structures on the lower slopes.

PSDM provides real dimensions of the large geological structures and salt structures imaged in all the deep central basins. The diapir imaged in the depth-migrated part of the CROP profile (Fig. 5) is almost 4 km high. Lateral salt flow to feed the diapir growth has caused lateral salt weld surfaces, namely the juxtaposition of UU directly on LU. Salt weld is commonly found around salt diapirs in both deep basins (Figs 3, 5, 6, 8, and 13b, c).

Salt detachment and downslope translation as a consequence of margin uplift and tilting is common in sedimentary basins (e.g. Hudec & Jackson 2004). The salt flow towards the basin occurs along a basal detachment and a series of growth faults that cause segmentation of the originally continuous salt layer. Such structures are particularly well imaged in the lower slope of the Gulf of Lions (Gorini *et al.* 2005; Lofi *et al.* 2005, 2011*a*), where not only the margin slope induced by basin subsidence, but also the sedimentary load of the Rhone deep-sea fan sediments have provided the driving force for salt gravity sliding and lateral spreading. Rollover structures are well developed at the base of the Sardinian slope, as the MSC units were continuously deposited both in the deep basins and its margin. The sedimentary load is probably the main driver in the Gulf of Lions, while margin tilting and gravity gliding are the dominant processes here. Only volcanic bodies (Fig. 6a) provide a local discontinuity of the MSC on the Sardinian slope. Less common are rollover structures on the South Balearic margin. The segmentation of the margin in marginal slope basins separated by steep fault scarps of the EBE has prevented the continuous salt deposition from the deep basin to its margin. The only rollover structures are found at the transition between the thin to thick salt basins below the Algero-Balearic abyssal plain.

Conclusions

The Sardo-Provençal and the Algero-Balearic sedimentary basins are floored by oceanic crust opened in different phases of back-arc extension in the Western Mediterranean and were fully open at the time of the Messinian Salinity Crisis (MSC). Therefore, during and after the MSC they were part of one continuous deep-water sedimentary basin. The Hannibal Ridge and a morphological step along the North Balearic Fracture Zone were probably the only submerged dividers between the two basins. The comparison between seismic stratigraphy and the MSC structures obtained by comparable seismic acquisition systems outlines the following characters.

The older basement age in Sardo-Provençal basin is reflected in a thicker pre-MSC sedimentary sequence than in the Algero-Balearic basin (1.7 and 0.97 km, respectively). In MSC and post-MSC times,

the younger Algero-Balearic basin should have undergone a higher subsidence rate than the older Sardo-Provençal basin according to the post-rift thermal subsidence curve, if the stretching factor of the two basin is the same. Because the MSC and later evolution of the sedimentary fill is comparable, a lower stretching factor must have characterized the opening of the Algero-Balearic basin.

The seismic record in the two deep basins is very similar in terms of seismic appearance, thickness and style of deformation of the MSC units. The similarity includes the presence of a thin salt layer within the upper part of the UU and a related intra-UU unconformity interpreted as a secondary base-level drop during the last phase of the MSC.

The style of salt deformation differs in the lower slope, as salt rollover structures are common on the West Sardinian margin, while they are less common on the South Balearic margin. Such difference is thought to be the result of a progressive subsidence and steepening on the Sardinian margin as opposed to a pre-MSC strike-slip system of the Emile Baudot Escarpment on the southern Balearic margin.

In the deep basins, salt structures are common and started to form already during the last phase of the MSC, at the time of deposition of UU. The most intense salt deformation was during the Early Pliocene. A progressive attenuation of halokinesis occurred throughout the Late Pliocene and Quaternary, with some evidence for present-day activity of the largest structures.

Acknowledgements and Funding

The authors gratefully acknowledge the anonymous reviewer for the constructive comments that were useful to improve the paper. The authors would also like to thank Paradigm for the use of the OGS academic licences of the Echoes and Geodepth processing software, IHS for the OGS and the University of Trieste free licences of the Kingdom Suite interpretation software and Schlumberger for the University of Trieste academic licence of the Petrel interpretation software. The seismic profiles of the Algero-Balearic margin were acquired within EUROFLEETS, call for ship-time 'Ocean' 2010, project 'Salt deformation and sub-salt fluid circulation in the Algero-Balearic abyssal plain – SALTFLU'. This work has been co-funded by the Flagship Project RITMARE, the Italian Research for the Sea, co-ordinated by the Italian National Research Council and funded by the Italian Ministry of Education, University and Research within the National Research Program 2011 – 13.

References

Acosta, J., Munoz, A., Herranz, P., Palomo, C., Ballesteros, M., Vaquero, M. *et al.* 2001. Geodynamics of the Emile Baudot Escarpment and the Balearic Promontory, Western Mediterranean. *Marine and Petroleum Geology*, **18**, 349–369.

Afilhado, A., Moulin, M. *et al.* 2015. Deep crustal structure across a young passive margin from wide-angle and reflection seismic data (The SARDINIA Experiment) – II. Sardinia's margin. *Bulletin de la Societé Géolgique de France*, **4–5**, 331–351.

Aslanian, D., Moulin, M. *et al.* 2012. Structure and evolution of the Gulf of Lions: the Sardinia Seismic Experiment and the GOLD (Gulf of Lions Drilling) project. *The Leading Edge - Special Section: Mediterranean Region*, **31**, 786–792.

Butler, R.W.H., Lickorish, W.H., Grasso, M., Pedley, H.M. & Ramberti, L. 1995. Tectonics and sequence stratigraphy in Messinian basins, Sicily: constraints on the initiation and determination of the Mediterranean salinity crisis. *Bulletin of the Geological Society of America*, **107**, 425–439.

Camerlenghi, A., Accettella, D., Costa, S., Lastras, G., Acosta, J., Canals, M. & Wardell, N. 2009. Morphogenesis of the SW Balearic continental slope and adjacent abyssal plain, Western Mediterranean Sea. *International Journal of Earth Sciences*, **98**, 735–750.

Carminati, E., Lustrino, M. & Doglioni, C. 2012. Geodynamic evolution of the central and western Mediterranean: Tectonics vs. igneous petrology constraints.*Tectonophysics*, **579**, 173–192, http://doi.org/10.1016/j.tecto.2012.01.026

Cherchi, A. & Montadert, L. 1982. Oligo Miocene rift of Sardinia and the early history of the Western Mediterranean Basin. *Nature*, **298**, 736–739.

CIESM 2008. *The Messinian Salinity Crisis from Mega-Deposits to Microbiology- A consensus report. In:* Briand, F. (ed.) CIESM Workshop Monographs, **33**. Monaco, 168.

Clauzon, G., Suc, J.P., Gautier, F., Berger, A. & Loutre, M.F. 1996. Alternate interpretation of the Messinian Salinity Crisis: controversy resolved? *Geology*, **24**, 363–366.

Cornée, J.J., Maillard, A., Conesa, G., García, F., Saint Martin, J.P., Sage, F. & Münch, P. 2008. Onshore to offshore reconstruction of the Messinian erosion surface in western Sardinia, Italy: MSC implications. *Sedimentary Geology*, **210**, 48–60.

Costa, E., Camerlenghi, A. *et al.* 2004. Modeling deformation and salt tectonics in the eastern Mediterranean Ridge accretionary wedge. *Geological Society of America Bulletin*, **116**, 880–894.

Dal Cin, M. 2014. *The Messinian Salinity Crisis: Seismic Interpretation in the North-Western Mediterranean Sea*. Master's thesis, University of Trieste, Trieste.

Decima, A. & Wezel, F.C. 1971. Osservazioni sulle evaporiti Messiniane della Sicilia centro-meridionale. *Rivista Mineraria Siciliana*, **130–134**, 172–187.

Déverchère, J., Yelles, K. *et al.* 2005. Active thrust faulting offshore Boumerdes, Algeria, and its relations to the 2003 Mw 6.9 earthquake. *Geophysical Research Letters*, **32**, L04311, http://doi.org/10.1029/2004GL021646

Domzig, A., Yelles, K. *et al.* 2006. Searching for the Africa–Eurasia Miocene boundary offshore western Algeria (MARADJA'03 cruise). *Comptes Rendus Geosciences*, **338**, 80–91, http://doi.org/10.1016/j.crte.2005.11.009

Driussi, O., Briais, A. & Maillard, A. 2015. Evidence for transform motion along the South Balearic margin and implications for the kinematics of opening of the Algerian basin. *Bulletin de la Societé Géolgique de France*, 2015, t. **186**, 353–370.

Fanucci, F. & Morelli, D. 2001. Characters and mechanisms of the Sardinian–Corsican Block drifting. *Studi Trentini di Scienze Naturali, Acta Geologica*, **77**, 5–14.

Feng, Y. E. & Reshef, M. 2016. The Eastern Mediterranean Messinian salt-depth imaging and velocity analysis considerations. *Petroleum Geoscience*, first published online August 17, 2016, http://dx.doi.org/10.1144/PETGEO2015-088

Finetti, I.R. (ed.) 2005. *CROP PROJECT: Deep Seismic Exploration of the Central Mediterranean and Italy*. Atlases in Geoscience, Elsevier B.V., **1**.

Finetti, I.R. & Morelli, C. 1973. Geophysical Exploration of the Mediterranean Sea. *Bollettino di Geofisica Teorica ed Applicata*, **15**, 263–341.

Finetti, I., Del Ben, A. *et al.* 2005. Crustal tectono-stratigraphic setting and geodynamics of the Corso-Sardinian Block from new CROP seismic data. *In:* Finetti, I. (ed.) *CROP PROJECT: Deep Seismic Exploration of the Central Mediterranean and Italy*. Atlases in Geoscience, **1**. Elsevier B.V., 430–446.

Gallart, J., Vidal, N., Estévez, A., Pous, J., Sábat, F. & Santisteban, C. & ESCI-Valencia Trough Group 1995. The ESCI-Valencia Trough vertical reflection experiment: a seismic image of the crust from the NE Iberian Peninsula to the Western Mediterranean. *Revista de la Sociedad Geológica de Espana*, **8**, 405–415.

Geletti, R., Zgur, F. *et al.* 2014. The Messinian Salinity Crisis: new seismic evidence in the West-Sardinian Margin and Eastern Sardo-Provençal Basin (West Mediterranean Sea). *Marine Geology*, **351**, 76–90.

Gorini, C., Lofi, J., Duvail, C., Tadeu Dos Reis, A., Guennoc, P., Lestrat, P. & Mauffret, A. 2005. The Late Messinian salinity crisis and Late Miocene tectonism: Interaction and consequences on the physiography and post-rift evolution of the Gulf of Lions margin. *Marine and Petroleum Geology*, **22**, 695–712.

Gueguen, E., Doglioni, C. & Fernandez, M. 1998. On the post 25 Ma geodynamic evolution of the western Mediterranean. *Tectonophysics*, **298**, 259–269.

Hsü, K.L., Ryan, W.F.B. & Cita, M.B. 1973. Late Miocene desiccation of the Mediterranean Sea. *Nature*, **242**, 240–244.

Hudec, M.R. & Jackson, P.A. 2004. Regional restoration across the Kwanza Basin, Angola: Salt tectonics triggered by repeated uplift of a metastable passive margin. *AAPG Bulletin*, **88**, 971–990.

Jones, I. F. & Davison, I. 2014. Seismic imaging in and around salt bodies. *Interpretation*, **2**, Society of Exploration Geophysicists and American Association of Petroleum Geologists, SL1–SL20.

Kallweit, R.S. & Wood, L.C. 1982. The limits of resolution of zero-phase wavelets. *Geophysics*, **47**, 1035.

Krijgsman, W., Hilgen, F.J., Raffi, I., Sierro, F.J. & Wilson, D.S. 1999. Chronology, causes and progression of the Messinian Salinity Crisis. *Nature*, **400**, 652–655.

Lofi, J., Gorini, C., Berné, S., Clauzon, G., Dos Reis, A.T., Ryan, W.B.F. & Steckler, M.S. 2005. Erosional processes and paleo-environmental changes in the Gulf of Lions (SW France) during the Messinian Salinity Crisis. *Marine Geology*, **217**, 1–30.

Lofi, J., Déverchère, J. *et al.* 2011*a*. *Atlas of the Messinian seismic markers in the Mediterranean and Black Seas*. Memoires Societe Geologique de France, n. s., **179** and World Geological Map Commission, **72**.

Lofi, J., Sage, F. *et al.* 2011*b*. Refining our knowledge of the Messinian salinity crisis records in the offshore domain through multi-site seismic analysis. *Bulletin de la Societé Géolgique de France*, **182**, 163–180.

Mauffret, A. 2007. The Northwestern (Maghreb) boundary of the Nubia (Africa) Plate. *Tectonophysics*, **429**, 21–44.

Mauffret, A., Maldonado, A. & Campilo, A. 1992. Tectonic frame work of the eastern Alboran and western Algerian basins (Western Mediterranean). *Geo-Mainer Letters*, **12**, 104–110.

Mauffret, A., Frizon de Lamotte, D., Lallemant, S., Gorini, C. & Maillard, A. 2004. E-W opening of the Algerian Basin (Western-Mediterranean). *Terra Nova*, **16**, 257–264.

McKenzie, D. 1978. Some remarks on the development of sedimentary basins. *Earth and Planetary Science Letters*, **40**, 25–32.

Mocnik, A., Camerlenghi, A., Del Ben, A., Geletti, R., Wardell, N. & Zgur, F. 2014. The Messinian Salinity Crisis in the West-Mediterranean Basins:

comparison between two rifted margins. *In*: Proceedings of the 33rd GNGTS Conference, Bologna, **1**, 156–163.

Montadert, L., Letouzey, J. & Mauffret, A. 1978. Messinian event: seismic evidence. *In:* Hsü, K.J. & Montadert, L. *et al.* (eds) *Initial Reports of the Deep Sea Drilling Project*, **1**. US Government Printing Office, Washington, DC, 1037–1050.

Moulin, M., Klingelhoefer, F. *et al.* 2015. Deep crustal structure across a young passive margin from wide-angle and reflection seismic data (The SARDINIA Experiment) – I. Gulf of Lion's margin. *Bulletin de la Societé Géolgique de France*, **4–5**, 309–330.

Rehault, J.P., Boillot, G. & Mauffret, A. 1984. The Western Mediterranean Basin geological evolution. *Marine Geology*, **55**, 447–477.

Reiche, S., Hübscher, C. & Beitz, M. 2014. Fault-controlled evaporite deformation in the Levant Basin, Eastern Mediterranean. *Marine Geology*, **354**, 53–68.

Rouchy, J.M. & Caruso, A. 2006. The Messinian salinity crisis in the Mediterranean basin: A reassessment of the data and an integrated scenario. *Sedimentary Geology*, **188–189**, 35–67.

Roveri, M., Lugli, S., Manzi, V. & Schreiber, C.B. 2008. *The shallow- to deep-water record of the Messinian Salinity Crisis: new insight from Sicily, Calabrian and Apennine basins*. *In:* Briand, F. (ed.) *CIESM Workshop Monographs*, **33**. Monaco, 73–82.

Roveri, M., Lugli, S., Manzi, V., Gennari, R. & Schreiber, B. 2014. High-resolution strontium isotope stratigraphy of the Messinian deep Mediterranean basins: Implications for marginal to central basin correlations. *Marine Geology*, **349**, 113–125.

Ryan, W.B.F. 2008. Modeling the magnitude and timing of evaporative drawdown during the Messinian salinity crisis. *Stratigraphy*, **5**, 227–243.

Ryan, W.B.F., Hsü, K.J. *et al.* 1973. Boundary of Sardinia slope with Balearic Abyssal Plain—Sites 133 and 134. *In:*Ryan, W.B.F., Hsü, K.J. *et al.* (eds) *Initial Reports of the Deep Sea Drilling Project*, **13**. US Government Printing Office, Washington, DC, **2**, 465–514.

Sàbat, F., Roca, E. *et al.* 1995. Role of extension and compression in the evolution of the eastern margin of Iberia: the ESCI-Valencia Trough seismic profile. *Revista de la Sociedad Geológica de España*, **8**, 431–448.

Sage, F., Von Gronefeld, G., Déverchère, J., Gaullier, V., Maillard, A. & Gorini, C. 2005. Seismic evidence for Messinian detrital deposits at the Western Sardinia Margin, Northwestern Mediterranean. *Marine and Petroleum Geology*, **22**, 757–773.

Scrocca, D., Doglioni, C. *et al.* 2003. CROP Atlas – Seismic Reflection Profiles of the Italian Crust. *Memorie descrittive della Carta Geologica d'Italia*, **62**, 194.

Steckler, M.S. & Watts, A.B. 1980. The Gulf of Lion: subsidence of a young continental margin. *Nature*, **287**, 425–430.

Wardell, N., Camerlenghi, A., Urgeles, R., Geletti, R., Tinivella, U., Giustiniani, M. & Accettella, D. 2014. Seismic evidence for Messinian salt deformation and fluid circulation on the South Balearic margin (Western Mediterranean). *Geophysical Research Abstracts,* EGU2014–11078–1.